Inorganic Chemistry

ARTICLE

pubs.acs.org/IC

Coordination Chemistry of *N*-Heterocyclic Stannylenes: A Combined Synthetic and Mössbauer Spectroscopy Study

Stephen M. Mansell,[†] Rolfe H. Herber,[*,‡] Israel Nowik,[‡] Douglas H. Ross,[†] Christopher A. Russell,[*,†] and Duncan F. Wass[†]

[†]School of Chemistry, University of Bristol, Cantock's Close, Bristol, #BS8 1TS, U.K.

[‡]Racah Institute of Physics, The Hebrew University of Jerusalem, 91904 Jerusalem, Israel

Supporting Information

ABSTRACT: The *N*-heterocyclic stannylenes (NHSns), [(Dipp)N(CH$_2$)$_n$N(Dipp)Sn] (Dipp = 2,6-^{i}Pr$_2$C$_6$H$_3$; n = 2, **1**; n = 3, **5**) and [(^{t}Bu)N(CHMe)$_2$N(^{t}Bu)Sn] (**10**) are competent ligands toward a variety of transition metal centers, as seen in the complexes [W(CO)$_5$·**1**] (**2**), [(OC)$_4$Fe(μ-**1**)$_2$Fe(CO)$_4$] (**3**), [(OC)$_4$Fe(μ-**1**)Fe(CO)$_4$] (**4**), [Fe(CO)$_4$·**5**]$_n$ (**6**, n = 1 or 2), [(OC)$_4$Fe(μ-**5**)Fe(CO)$_4$] (**7**), [Ph$_3$PPt(μ-**1**)$_2$PtPPh$_3$] (**8**), [Fe(CO)$_4$·**10**] (**11**), and [(η^5-C$_5$H$_5$)(OC)$_2$Mn·**10**] (**12**). X-ray crystallographic studies show that the NHSns are structurally largely unperturbed binding to the metal, but in contrast to the parent NHCs, NHSns often adopt a bridging position across dinuclear metal units. The balance between terminal and bridging positions for the stannylene is evidently closely balanced as shown by the observation of both monomers and dimers for **6** in the solid state and in solution. ^{119}Sn and ^{57}Fe Mössbauer spectroscopy of the complexes shows the tin atoms in such complexes to be consistent with electron deficient Sn(II) centers.

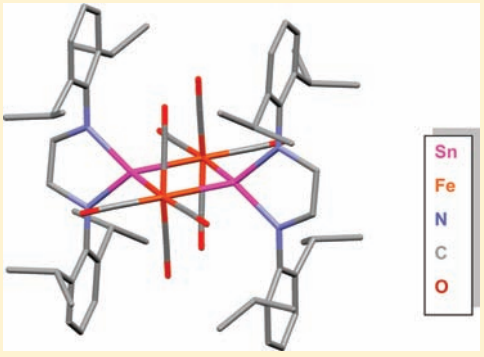

INTRODUCTION

N-heterocyclic carbenes (NHCs) are one of the most intensely studied classes of compounds in the past two decades.[1] A vast body of work has been published on their fascinating chemistry since the first report of their isolation as stable species,[2] including, notably, their ability to act as ligands in catalytically active systems.[3] More recently, they have attracted attention because of their ability to form and stabilize highly unusual main group species.[4] In seeking to modify the NHC unit, chemists have adopted a series of strategies such as changing the substituents on the nitrogen atoms,[1c,5] varying the backbone of the ligand,[6] or through use of a chiral scaffold.[7] An alternative strategy involves exchange of one or both of the *N*-centers for other units, leading, for example, to cyclic alkyl-amino carbenes[8] or *P*-heterocyclic carbenes,[9] which themselves have demonstrated rather different but exciting new chemistry.[8b] Our own interest and those of several other groups[10] has focused on exchanging the carbene carbon atom for other isovalent units. Representative examples have been reported of ionic species containing donor atoms from group 13,[11] group 15,[12] and even group 16.[13] In addition, there is a rich chemistry reported for the neutral group 14 homologues of carbenes, a topic where initial reports[14] predate the discovery of NHCs by a considerable number of years.[15] The chemistry of these group 14 *N*-heterocyclic carbene analogues has focused largely on the lighter congeners which are *N*-heterocyclic silylenes[16] and *N*-heterocyclic germylenes,[16e,17] but recent reports have extended this to the two heaviest elements in the group.[17d,17e,18] These were prepared by the salt metathesis of the appropriate dilithiated diamide with MCl$_2$ (M = Sn, Pb) and showed a high degree of thermal stability compared to the corresponding species with unsaturated backbones.[18b,18d] The degree of aggregation displayed by these species was closely related to the steric bulk of the substituents on the N centers.

Alongside reports of the preparation of these low-valent, low-coordination number species has been an exploration of their coordination chemistry, in particular toward the transition elements. The parent NHCs are classed as being extremely strong σ-donors, with π-acceptance being of much less importance.[19] Almost all structurally characterized examples of NHCs bonded to metal atoms display terminal coordination through the carbene lone pair although a few examples of abnormal bonding through another carbon atom in the heterocyclic ring have been observed.[20] Examples of NHCs which bridge metal centers are very rare with a search of the Cambridge Structural Database revealing only 12 examples of bridging coordination.[21] In each case, the formation of bridging carbenes is observed where the NHC is part of a multidentate ligand, with the bridging position being adopted

Received: September 20, 2010
Published: February 14, 2011

Scheme 1. Coordination of *N*-Heterocyclic Stannylenes to Transition Metal Fragments (R = 2,6-$^{i}Pr_2C_6H_3$)

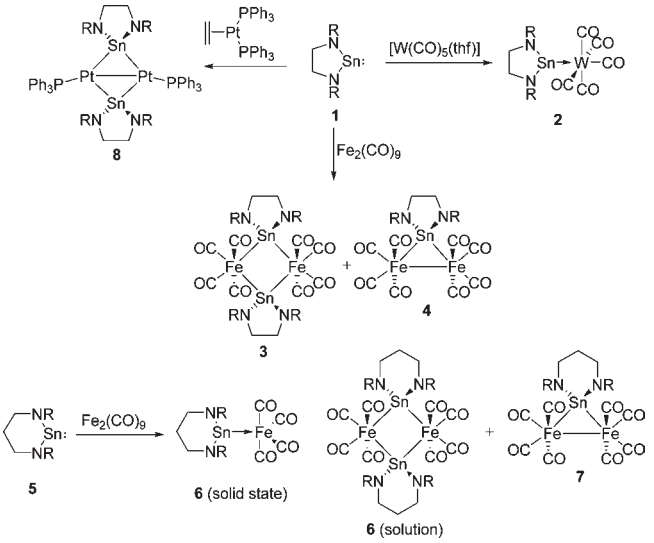

as a consequence of the geometric constraints of the multidentate ligand rather than an express preference for a bridging position.[22]

The heavier homologues of NHCs have a much less well-developed coordination chemistry than *N*-heterocyclic carbenes.[23] *N*-heterocyclic silylenes are usually observed as a terminal ligand, although the bridging mode has been identified with Pd(0) precursors.[24] The coordination chemistry of other (non NHC type) silylene complexes formed at a transition metal center are reviewed elsewhere.[25] Similarly, *N*-heterocyclic germylenes have been shown to coordinate terminally to a range of transition metal centers, all in a terminal bonding mode.[17a,17b,26] The coordination chemistry of *N*-heterocyclic stannylenes, the subject of this report, is also relatively under explored. Homoleptic nickel(0) complexes of a *N*-heterocyclic stannylene were reported in 1990,[27] but the wider field of coordination complexes of other stannylene ligands dates back still further. In this regard we note the pioneering work of the groups of Lappert and Veith probing the chemistry of a variety of stannylenes, for example, $[Sn\{E(SiMe_3)_2\}_2]$ (E = N, CH)[23b] and $[Sn\{N(^{t}Bu)\}_2SiMe_2]$,[28] showing them to be versatile ligands to a range of transition metal centers. Hahn et al. have recently prepared and explored the coordination chemistry of benzannulated *N*-heterocyclic stannylenes, preparing chelating bis(stannylene) complexes of Ni(0),[29] Pt(0),[30] and Mo(0) and using computational chemistry to investigate the σ/π-donor and π-acceptor effects.[31]

In this study, we sought to investigate the coordination chemistry of a class of *N*-heterocyclic stannylenes which we recently reported containing saturated organic backbones and probe the metal−ligand interaction using X-ray crystallography, NMR spectroscopy, and Mössbauer spectroscopy. In addition, we describe a new and rare example of a chiral NHSn and investigate its coordination chemistry.

RESULTS AND DISCUSSION

Bridging and Terminal Coordination of *N*-Heterocyclic Stannylenes. To probe the coordination chemistry of *N*-heterocyclic stannylenes, a number of complexes were prepared by reaction of the free *N*-heterocyclic stannylene with transition metal species bearing labile ligands (Scheme 1). Coordination of the stannylene results in a downfield shift of the ^{119}Sn chemical shift (these are collated in Table 1; NMR data collected for other nuclei are detailed within the Experimental Section for the specific compound). The products are extremely air- and moisture-sensitive but are generally quite thermally stable in the solid state, with some samples showing no signs of decomposition until above 200 °C. In this report, we will discuss each compound in turn before analyzing the Mössbauer spectroscopy results separately.

Table 1. ^{119}Sn Chemical Shifts of Complexes 2, 3, 6, 8, 11, and 12 and Comparison to Those of the Respective Free Stannylene

compound	^{119}Sn chemical shift (multiplicity)[a]	^{119}Sn chemical shift of free stannylene
2	426.2 (s with ^{183}W satellites $^{1}J(^{119}Sn-^{183}W)$ = 1150 Hz)	366
3	525.3 (s)	366
6	498.0 (s)	291
8	500 (br. s)	366
11	534.0 (s)	454
12	625 (br. s)	454

[a] 112 MHz, 25 °C, C_6D_6

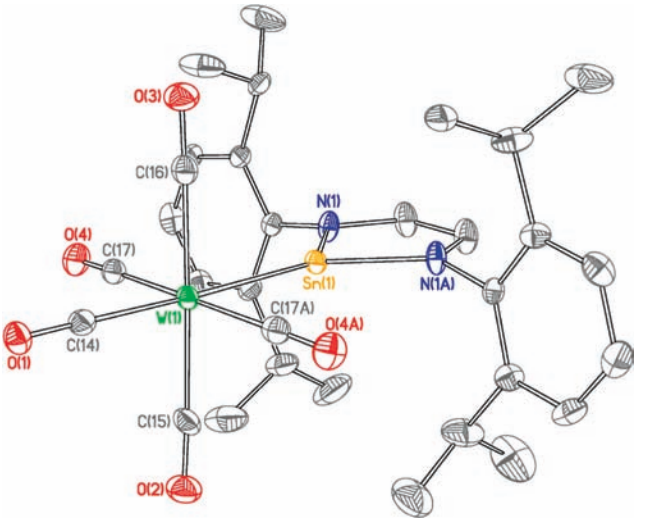

Figure 1. Thermal ellipsoid plot of **2**. All hydrogen atoms have been removed for clarity, and thermal ellipsoids are set at 30% probability. Selected bond lengths (Å) and angles (deg): Sn1−W1 2.6889(3), Sn1−N1 1.994(2), Sn1−N1A 1.993(2); N1−Sn1−N1A 83.57(13); $\sum$ (angles at N1) 358.7.

Reaction (thf, r.t., 16 h) of $[Sn\{N(Dipp)CH_2\}_2]$ (**1**) with the distinctive bright yellow colored $[W(CO)_5(thf)]$ (Scheme 1) gave a deep red solution. ^{119}Sn NMR spectroscopy showed a singlet at high frequency (Table 1) with ^{183}W satellites. Recrystallization of **2** from *n*-hexane gave X-ray quality crystals which showed the stannylene binding through the Sn center to the $W(CO)_5$ fragment (Figure 1).

In complex **2**, the stannylene ring, which as a free species adopts a non-planar conformation in the solid state, becomes planar on coordination, a feature which has also been observed for a number of saturated NHCs.[32] Other dimensions of the stannylene remain largely unaltered upon complexation.

dx.doi.org/10.1021/ic101920x |*Inorg. Chem.* 2011, 50, 2252–2263

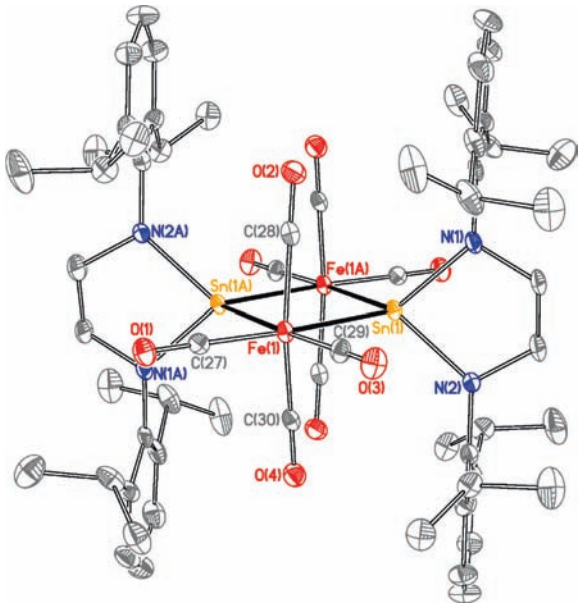

Figure 2. Thermal ellipsoid plot of **3**. All hydrogen atoms have been omitted for clarity, and thermal ellipsoids are set at 30% probability. Selected bond lengths (Å) and angles (deg): Sn1−N1 2.041(3), Sn1−N2 2.045(3), Sn1−Fe1A 2.6688(7), Sn1−Fe1 2.6689(7), Fe1−Sn1A 2.6686(7); N1−Sn1−N2 84.08(14), Fe1A−Sn1-Fe1 98.640(17), Sn1A−Fe1-Sn1 81.358(17); ∑ (angles at N1) 359.3, ∑ (angles at N2) 359.8.

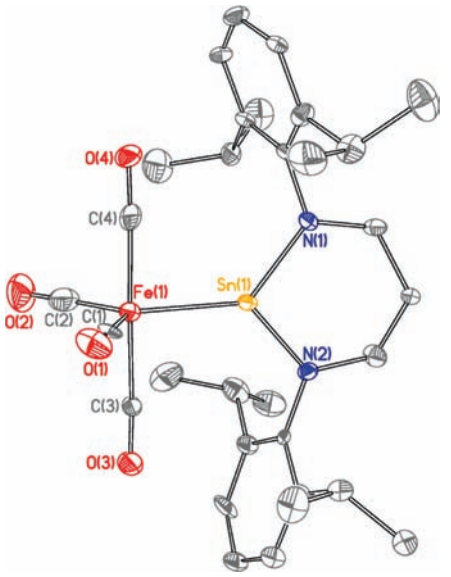

Figure 3. Thermal ellipsoid plot of one of the two crystallographically independent molecules in the asymmetric unit of **6**. All hydrogen atoms have been omitted for clarity, and thermal ellipsoids are set at 50% probability. Selected bond lengths (Å) and angles (deg) for both molecules: Sn1−N2 1.990(4), Sn1−N1 1.998(5), Sn1−Fe1 2.4299(10), Sn2−N3 2.008(4), Sn2−N4 2.018(5), Sn2−Fe2 2.4293(10); N2−Sn1−N1 97.12(19), N3−Sn2−N4 94.9(2); ∑ (angles at N1) 359.9, ∑ (angles at N2) 359.6, ∑ (angles at N3) 360.0, ∑ (angles at N4) 359.7.

In C_6D_6 solution, the ^{1}H NMR spectrum of **2** showed inequivalent methyl groups within each *iso*-propyl substituent; furthermore the backbone CH_2 protons were observed as singlets together with poorly resolved satellites with about 22 Hz coupling arising from ^3J coupling to the ^{119}Sn and ^{117}Sn nuclei; this feature was not resolved in the free stannylene. ^{13}C NMR spectroscopy revealed CO resonances at 197.7 and 194.4 ppm (cf. $W(CO)_6$ at 192 ppm[33]) with the much less intense signal at 197.7 ppm tentatively assigned to the *trans* carbonyl. IR spectroscopy in *n*-hexane solution showed three CO stretches at 2076.2, 1960.4, and 1928.7 cm^{-1}. These stretches are similar to the a_1 bands of the corresponding $W(CO)_5$ complexes of $[Sn\{N(SiMe_3)_2\}_2]$ (2073, 1931 cm^{-1}), PPh_3 (2075, 1938 cm^{-1}), and an *N*-heterocyclic carbene (2060, 1927 cm^{-1}),[34] suggesting that the NHSn has similar net donor/acceptor properties to these other ligands.

An alternative coordination mode for **1** was revealed from the equimolar reaction (16 h, r.t., toluene) with $[Fe_2(CO)_9]$ (Scheme 1). Bright red crystals of the product, **3**, were grown from *n*-hexane, and X-ray crystallography showed them to contain a diamond-shaped Fe_2Sn_2 core (Figure 2), with non-planar SnN_2C_2 rings perpendicular to the Fe_2Sn_2 plane. The stannylene units are relatively unfettered by complexation, with comparatively short Sn−N bonds {2.041(3) and 2.045(3) Å} which are only marginally longer than in both the free stannylene and in complex **2**, and planar nitrogen centers. The Fe−Sn distances {which are symmetry imposed to be equal at 2.6689(7) Å} are slightly longer than for non-bridging iron-stannylene complexes (vide infra), while both the Fe−C and CO bonds are all identical within error.

The related reaction (toluene, r.t., 16 h) of a *N*-heterocyclic stannylene with a three-carbon backbone (**5**) with $[Fe_2(CO)_9]$ (Scheme 1) proceeded in an apparently similar manner, giving a dark orange/red solution. However, crystals of **6** grown from toluene had a yellow coloration, and a single crystal X-ray diffraction study showed a rather different solid-state structure (Figure 3).

The stannylene was observed to coordinate in a terminal manner to a $Fe(CO)_4$ fragment, adopting an equatorial position with the stannylene parallel to the axial carbonyl ligands. The Sn−Fe distances {2.430(1) and 2.429(1) Å for each of the independent molecules in the unit cell} are short compared to literature values {av. Fe−Sn distance is 2.56(7) Å},[35] although we note a series of examples where similarly short Sn−Fe contacts have been observed, for example, in a bis(aryloxide)stannylene-$Fe(CO)_4$ compound (2.408(1) Å);[36] $[(toluene)Fe(SnAr_2)_2]$ {2.432(1) and 2.434(1) Å};[37] and 2.436(1) Å in $[(toluene)Fe(C_2H_4)SnAr_2]$.[38] The Sn−N bond lengths {1.990(4) to 2.018(5) Å} are similar to those in the free stannylene,[18d] and the N centers are planar (sum of angles at all N atoms above 359.6°). However, the difference in color between the observed solid-state crystals and in solution led us to probe the solution behavior in more detail. NMR spectroscopy data (+25 °C, C_6D_6) for both **3** and **6** are similar with sharp peaks seen in the ^{119}Sn NMR spectra at δ = 525.3 ppm (**3**) and 498.0 ppm (**6**). These are both shifted to higher frequency (and are much sharper) than those seen in the respective free stannylenes (366 ppm for **1** and 291 ppm for **5**).[18d] ^{1}H NMR spectroscopy revealed two doublets and one septet for the *iso*-propyl groups and unresolved coupling to ^{119}Sn/^{117}Sn was seen for the CH_2 group in **3**. ^{13}C NMR spectroscopy revealed peaks diagnostic of the coordinated stannylene ligands as well as a single peak for the CO ligands at δ = 212.6 ppm in **3** and 212.5 ppm in **6**. To determine whether the bridging or terminal structure is adopted in solution for either compound, DOSY experiments were performed on C_6D_6 solutions of both complexes (Table 2). Diffusion constants of 5.036×10^{-10} m^2 s^{-1} for **3** and 4.951×10^{-10} m^2 s^{-1} for **6** were obtained and through the use of the Stokes−Einstein equation

dx.doi.org/10.1021/ic101920x |*Inorg. Chem.* 2011, 50, 2252–2263

Table 2. Structures of the Iron−Tin Complexes 3 and 6 in Solution and the Solid State

crystal structure			DOSY experiments		
compound	volume/Å^3	radius/Å	diffusion coefficient/m^2 s^{-1}	calculated hydrodynamic radius/Å	solution structure
3 (dimer)	1289.0	6.75	5.036×10^{-10}	6.7	dimer
6 (monomer)	694.5	5.5	4.951×10^{-10}	6.8	dimer

($D = kT/6\pi\eta R_H$, k = Boltzmann constant, η = viscosity of C_6D_6 at 25 °C: 6.46×10^{-4} kg m^{-1} s^{-1},[39] R_H = hydrodynamic radius), the hydrodynamic radii of the species were calculated; 6.7 Å for **3** and 6.8 Å for **6**. It is evident from the results that the molecules are of a very similar size in solution and through calculating the crystallographic radius from the crystal structure volume, (5.5 Å for **6** and 6.75 Å for **3**), it is seen that both compounds are dimeric in solution.

IR spectroscopy of **3** in *n*-hexane showed CO stretches at 2091.8, 2039.9, 2014.6, and 1962.2 cm^{-1} and very similar absorptions in the solid state. In contrast, *n*-hexane solutions of **6** gave stretches at 2061.5, 2052.1, 1990.2, and 1970.0 cm^{-1} and a rather different set of absorptions in the solid state (2089.8, 2059.7, 2042.9, 2021.4, 1966.9, and 1940.7 cm^{-1}), thus corroborating the other evidence of different structures in solution and the solid state.

In light of this observation that alternative structures are accessible for **6** in the solid state and in solution, a detailed re-examination of a crystalline sample from the reaction of **5** with [$Fe_2(CO)_9$] was undertaken. This revealed that indeed, a very small number of red crystals were present among the bulk of yellow crystals of **6**. X-ray diffraction experiments revealed the structure of this minor product, **7**, to contain a bridging stannylene ligand, but this time only one bridging an Fe−Fe bond between $Fe(CO)_4$ units (Figure 4).

The analysis of its solid-state structure is complicated by the presence of four crystallographically independent molecules in the asymmetric unit. However, the majority of bond dimensions are comparable to those seen in the other Fe-stannylene complexes **3**, **4**, and **6**.

A detailed re-examination of the ^{1}H NMR spectrum from the reaction mixture showed **6** as the major product as well as another set of very minor peaks that are consistent with the structure of **7**. Peaks at 3.87 (septet), 3.02 (multiplet), and 1.50 ppm (doublet) were assigned to **7**, with the remaining resonances not being identified as they presumably overlap with the dominant signals from the major product, **6**.

The different bonding modes apparent for stannylene **5** in complexes **6** and **7** led us to speculate whether the same variability may be observed for other stannylenes. Hence we reviewed the ^{1}H NMR spectroscopic data from the crude reaction mixture used to isolate **3** which revealed a minor set of peaks with signals at 3.96 (septet), 3.50 (singlet), and 1.48 ppm (doublet) which may correspond to a minor product **4**. Crystallization of the mother liquor after initial crystallization of **3** led to material that was mostly free diamine, Dipp(H)NCH$_2$CH$_2$N(H)Dipp. However, a few red crystals of **4** were observed in the mixture and were suitable for analysis by X-ray crystallography, and the molecular structure of this product was obtained (Figure 5). Unfortunately, this is the only unequivocal data on this pure compound as contamination with the free diamine, the very small yields, and the high air- and moisture-sensitivity of all the compounds involved prevented us from acquiring complete analytical data for **4**.

The molecular structure was very similar to that of **7**, with a single stannylene ligand bridging two $Fe(CO)_4$ fragments which

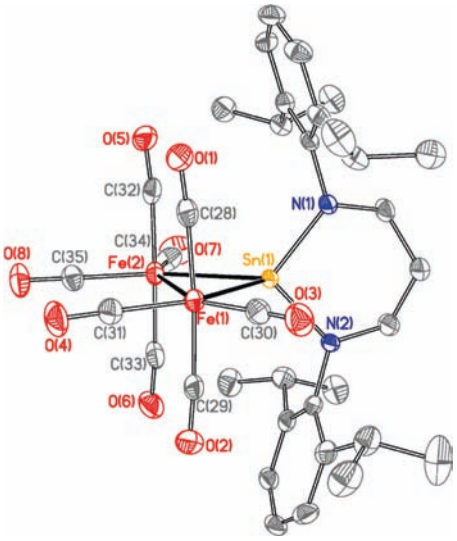

Figure 4. Thermal ellipsoid plot of one of the four crystallographically independent molecules in the asymmetric unit of **7**. All hydrogen atoms have been removed for clarity, and thermal ellipsoids are set at 50% probability. Selected bond lengths (Å) for all four molecules and selected angles for a representative molecule (deg): Sn1−N1 2.026(2), Sn1−N2 2.037(2), Sn1−Fe2 2.5734(4), Sn1−Fe1 2.5764(4), Fe1−Fe2 2.8572(5), Sn2−N4 2.034(2), Sn2−N3 2.032(2), Sn2−Fe4 2.5664(4), Sn2−Fe3 2.5769(4), Fe3−Fe4 2.8557(5), Sn3−N6 2.022(2), Sn3−N5 2.036(2), Sn3−Fe5 2.5464(4), Sn3−Fe6 2.5901(4), Fe5−Fe6 2.8600(5), Sn4−N8 2.030(2), Sn4−N7 2.036(2), Sn4−Fe7 2.5697(4), Sn4−Fe8 2.5798(4), Fe7−Fe8 2.8571(5); N1−Sn1−N2 96.64(8), Fe2−Sn1−Fe1 67.40(1); $\sum$ (angles at N1) 358.8, $\sum$ (angles at N2) 359.2.

appear to be linked with an Fe−Fe bond. The Sn−N bonds are similar to those previously seen in **1**−**3**, and the nitrogen atoms are planar. In contrast to **7**, the bridging stannylene leans significantly more toward one iron center than the other, although the reason for this is not readily apparent.

The bridging stannylene motif across Fe−Fe vectors in **3**, **4**, and **7** was also seen using other metals. Reaction of **1** with [$(Ph_3P)_2Pt(C_2H_4)$] gave a red solution, and crystals suitable for X-ray crystallography were grown from benzene. This showed **8** as containing a butterfly shaped Sn_2Pt_2 core with two stannylene units bridging the Pt−Pt vector of a $(Ph_3P)Pt-Pt(PPh_3)$ fragment (Figure 6). The SnN_2C_2 rings are twisted, with the SnN_2 unit lying at an angle of 73.2° to the Sn_2Pt plane, in contrast to the orthogonal arrangement seen in **3**. The Sn−N bonds are short and slightly unsymmetrical {2.043(2) and 2.028(2) Å} and the nitrogen atoms are planar. The Sn−Pt distances are short and similar {the unique distances are 2.6096(2), 2.5995(2), and 2.5994(2) Å} and the angle between the Pt1−Sn1−Pt1A and Pt1−Sn1A−Pt1A planes is 153.4°, in contrast to the planar arrangement (i.e., 180°) seen in **3**. Unusually, the PPh_3 ligands pendant to the Pt centers adopt a markedly *cisoid* orientation about the Pt−Pt vector, the distance of which is 2.6393(2) Å, and is consistent with a single bond.[40] We note that other tin species

dx.doi.org/10.1021/ic101920x |*Inorg. Chem.* 2011, 50, 2252–2263

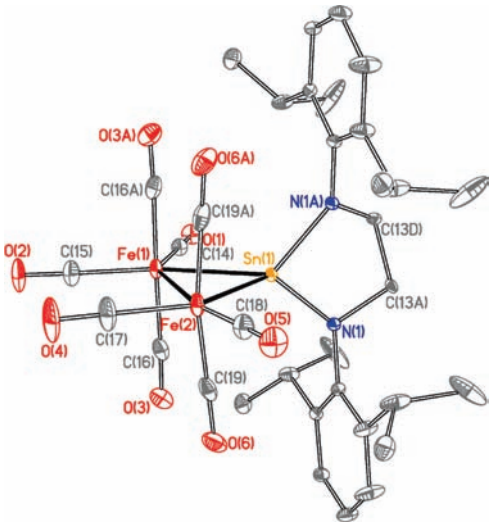

Figure 5. Thermal ellipsoid plot of **4**. All hydrogen atoms have been removed for clarity, and thermal ellipsoids are set at 30% probability. The carbon atoms forming the backbone of the stannylene ligand (C13) are disordered over two sites and only one set is displayed. Selected bond lengths (Å) and angles (deg): Sn1−N1 2.0205(18), Sn1−N1A 2.0205(18), Sn1−Fe1 2.5739(5), Sn1−Fe2 2.5296(5), Fe1−Fe2 2.8965(7); N1A−Sn1−N1 84.23(10).

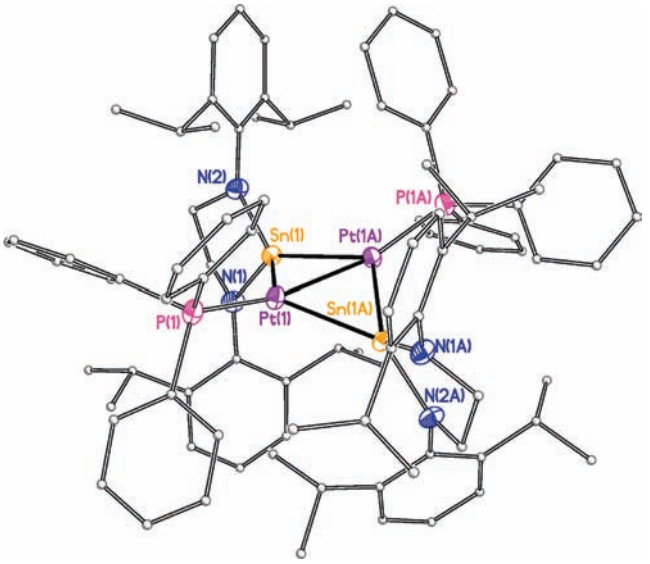

Figure 6. Thermal ellipsoid plot of **8**. All hydrogen atoms and the three benzene solvate molecules have been removed for clarity. The thermal ellipsoids for the Sn, Pt, N, and P atoms are set at 50% probability, while the C atoms are represented as spheres of 0.1 Å radius. Selected bond lengths (Å) and angles (deg): Pt1A−Sn1 2.5994(2), Pt1−Sn1 2.6096(2), Pt1A−Pt1 2.6392(2), Sn1−N2 2.027(2), Sn1−N1 2.043(2), Sn1−Pt1A 2.5995(2); Sn1A−Pt1-Sn1 114.078(6), P1−Pt1−Pt1A 165.30(2), N2−Sn1−N1 83.10(9), Pt1A−Sn1−Pt1 60.882(6); ∑ (angles at N1) 358.3, ∑ (angles at N2) 358.0.

have been reported to bridge both homonuclear Pd and Pt bonds,[41,26b] although the precise arrangement identified in **8** is unique.

^{1}H NMR spectroscopy revealed sharp signals for the stannylene units with a notably large difference in chemical shift between the nonequivalent CH*Me*$_2$ environments of 0.22 ppm (cf. 0.07 ppm in both **1** and **2**). ^{31}P NMR spectroscopy revealed a broad resonance at 52.0 ppm with broad ^{195}Pt satellites (5173 Hz) but with no discernible coupling to tin; heating the sample to 60 °C did not cause any further sharpening of the signal. ^{119}Sn NMR spectroscopy of this complex (Table 1) only revealed an extremely broad signal at about 500 ppm, possibly on account of coupling to the multiple spin-active nuclei in the complex.

Scheme 2. Synthesis and Coordination Chemistry of a Chiral *N*-Heterocyclic Stannylene[a]

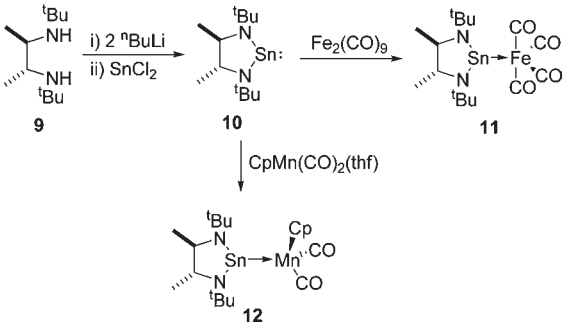

[a] All compounds shown were formed as racemic mixtures.

In summary, these results show that NHSns have a propensity to adopt bridging coordination modes. Relative to NHCs, the heavier analogues generally possess a more inert lone pair of electrons in a nominal sp^2-hybrid orbital and a reactive, Lewis acidic empty p-orbital.[10] The Lewis-acidity of the empty p-orbital often leads to dimerization or oligomerization of NHSns[18d,42] via interactions of the divalent atom with ring-nitrogen donors of adjacent molecules. Presumably the observation of bridging modes for NHSns across transition metal vectors is a manifestation of the same effect.

Synthesis and Coordination Chemistry of a Chiral *N*-Heterocyclic Stannylene. Given the importance of chiral ligands in enantioselective reactions, we were keen to explore the synthesis of chiral *N*-heterocyclic stannylenes.[43] This was achieved by dilithiation of chiral diamine **9** and reaction with $SnCl_2$ at low temperature in diethyl ether (Scheme 2).

The analogous silylene has been reported by reduction of a dihalodiaminosilane, and interesting chemistry of this species has been reported.[44] Crystals of **10** suitable for X-ray crystallography revealed the monomeric nature of the stannylene (Figure 7) with both enantiomers present in the asymmetric unit. The two molecules in other respects are very similar, with symmetric Sn−N bonds varying between 2.019(4) and 2.039(4) Å and planar nitrogen atoms. No close intermolecular contacts were found akin to those in **1**, which is unsurprising given the absence of aryl groups in **10**.[18d] In other respects the stannylenes show similar physical attributes, with compound **10** subliming at 0.5 Torr and 100 °C (compared to 160 °C at 7.5×10^{-5} Torr for **1** and 200 °C at 1×10^{-2} Torr for **5**), and displays thermochromic behavior as solutions of the stannylene frozen in *n*-hexane at −196 °C are bright red, whereas at room temperature the stannylene is yellow.[18d] ^{1}H NMR spectroscopy showed a sharp singlet for the *tert*-butyl group, a doublet for the methyl group, and a quartet for the CH protons. ^{119}Sn NMR spectroscopy showed a singlet resonance at 454 ppm, consistent with a two-coordinate tin center.

The coordination chemistry of this chiral *N*-heterocyclic stannylene was then probed by reaction with $[Fe_2(CO)_9]$ in toluene to afford a direct comparison with the coordination behavior of

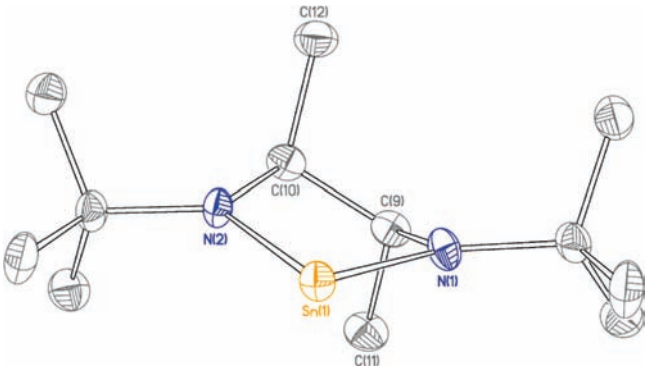

Figure 7. Thermal ellipsoid plot of one of the two molecules (the *S*,*S* enantiomer is shown; the other molecule in the asymmetric unit is the *R*, *R* enantiomer) in the asymmetric unit of **10**. All hydrogen atoms have been removed for clarity and thermal ellipsoids are set at 50% probability. Selected bond lengths (Å) and angles (deg): Sn1−N2 2.019(4), Sn1−N1 2.038(4), Sn2−N3 2.033(5), Sn2−N4 2.039(4), N2−Sn1−N1 82.05(17), N3−Sn2−N4 81.97(18); ∑ (angles at N1) 360.0, ∑ (angles at N2) 359.7, ∑ (angles at N3) 359.6, ∑ (angles at N4) 360.0.

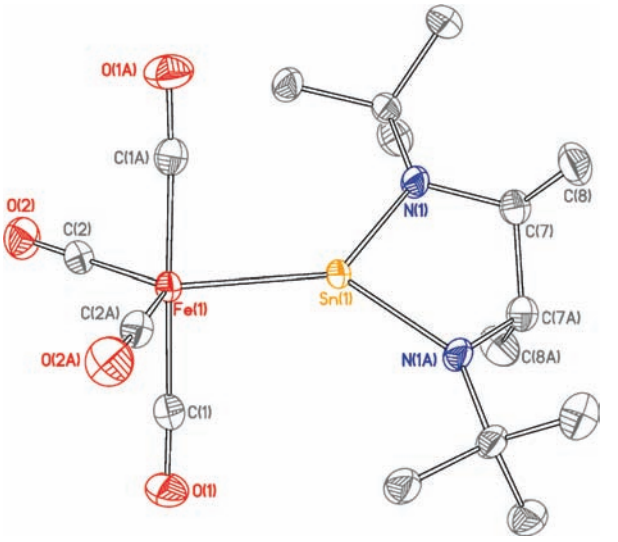

Figure 8. Thermal ellipsoid plot of **11**. All hydrogen atoms have been removed for clarity, and thermal ellipsoids are set at 50% probability. Selected bond lengths (Å) and angles (deg): Sn1−N1 2.0127(16), Sn1−Fe1 2.4683(4); N1−Sn1−N1A 84.65(9); ∑ (angles at N1) 359.7.

non-chiral NHSns. Crystallization of the product from *n*-hexane afforded **11** as red crystals which X-ray crystallographic experiments showed to contain terminal coordination of the stannylene to the $Fe(CO)_4$ fragment in the equatorial position with a 2-fold rotation axis running through the Fe−Sn bond (Figure 8). In contrast to **6**, the N−Sn−N plane does not lie in the plane of the axial carbonyl ligands, being significantly twisted (by 40.3°) away from this plane. The Fe−Sn bond is marginally longer {2.4683(4) Å} than the bond lengths seen in **6** {2.430(1) and 2.429(1) Å}. However, the Sn−N bond lengths {2.0127(16) Å} remain very short and the N−Sn−N angle {84.65(9)°} is only slightly more open than that seen in the free stannylene {82.05(17) and (81.97(18)°}.

As expected, coordination of the stannylene results in a downfield shift in the ^{119}Sn NMR chemical shift (Table 1), and ^{1}H NMR spectroscopy of **11** showed similar signals compared to the free stannylene **10**, but with unresolved ^{119}Sn and ^{117}Sn satellites with ^{3}J coupling of about 36 Hz now observed, as seen for the other stannylene complexes.

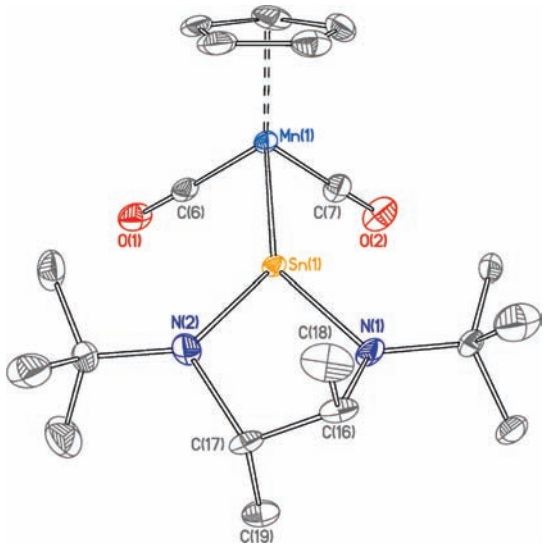

Figure 9. Thermal ellipsoid plot of **12**. All hydrogen atoms have been removed for clarity, and thermal ellipsoids are set at 30% probability. Only one position for each of the carbon atoms in the disordered stannylene backbone (C16, C17, C18 and C19) is shown. Selected bond lengths (Å) and angles (deg): $Cp_{centroid}$−Mn1 1.774, Mn1−Sn1 2.4705(4), Sn1−N1 2.013(2), Sn1−N2 2.013(2), N1−Sn1−N2 83.52(10); ∑ (angles at N1 for component shown) 353.2, ∑ (angles at N2 for component shown) 354.5.

Coordination of the chiral stannylene was also observed by reaction with $[CpMn(CO)_2(thf)]$, generated by photolytic cleavage of $[CpMn(CO)_3]$ in thf. The dark red color of $[CpMn(CO)_2(thf)]$ faded and the orange product (**12**) was recrystallized from *n*-hexane. A structural study was carried out using X-ray crystallography and revealed terminal coordination of the *N*-heterocyclic stannylene to the manganese center (Figure 9). The stannylene remains puckered and appears relatively unperturbed by coordination to the Mn center. ^{119}Sn NMR spectroscopy (Table 1) showed a very broad resonance at 625 ppm, with the broadness probably being a consequence of coupling to the quadrupolar manganese atom (^{55}Mn, 100% $I = 5/2$).

■ MÖSSBAUER SPECTROSCOPY STUDIES

Compound 1. In common with the other samples investigated in this study (with the exception of **6**) the ^{119}Sn ME spectra consist of doublets, and evidence more than one Sn atom site. In the case of **1**, these two sites consist of a major and minor spectral contribution, the latter presumably due to a byproduct or the result of minor sample degradation prior to examination. In any event, the major site in **1** evidence an isomer shift (I.S.) of 2.27 ± 0.01 mm sec^{-1} and a quadrupole splitting (Q.S.) of 2.25 ± 0.04 mm sec^{-1} at 90 K, indicative of the expected Sn(II) nature of the metal center, with a major contribution to the Q.S. arising from the lone pair. A representative spectrum is shown in Supporting Information, Figure S1, and the hyperfine and derived parameters are summarized in Table 3. The I.S. of the minor constituent is nearly the same as that of the major one, but the Q.S. parameter is smaller by ∼38%, strongly suggesting a different ligation mode of the tin atom in the minor constituent, supportive of our hypothesis of the dimeric form

dx.doi.org/10.1021/ic101920x |*Inorg. Chem.* 2011, 50, 2252–2263

Table 3. ^{119}Sn and ^{57}Fe Mössbauer Data for Compounds 1−3, 5, and 6[a]

compound/param	1	2	3	5	6	units
IS(90) (Sn)	2.271(2)	1.652(12)	1.926(48)	2.173(6)	1.53(2)	mm s^{-1}
QS(90) (Sn)	2.460(20)	2.812	2.801	2.279(6)	0.986(52)	mm s^{-1}
IS(90) (Fe)			−0.024(5)		−0.012(4)	mm s^{-1}
QS (90) (Fe)			1.866(5)		0.49(4)	mm s^{-1}
$k^2\langle x_{ave}^2\rangle_M$ (Sn)	2.60	2.07	2.76(2)	3.74(1)	1.65(11)	
$k^2\langle x_{ave}^2\rangle_X$ (Sn)	3.87	3.56	2.41(3)	4.48(1)	2.56(3)	
$k^2\langle x_{ave}^2\rangle_M$ (Fe)			1.040(13)		1.17(10)	
$k^2\langle x_{ave}^2\rangle_X$ (Fe)			1.048(18)		1.09(3)	

[a] The values in parentheses indicate the experimental error in the last digit(s).

of **1**. The area ratio of the two sites at 90 K is ∼3:1, and this ratio is not a sensitive parameter, consistent with the organometallic natures of the two sites.

As noted earlier,[45] the temperature-dependence of the recoil-free fraction, *f*, for an optically thin absorber, as derived from the temperature-dependence of the area under the resonance curve, can be expressed by the parameter $\mathbf{F}_{M.T} = k^2\langle x_{ave}^2\rangle$, where *k* is the wave vector of the appropriate ME radiation, and $\langle x_{ave}^2\rangle$ is the mean-square-amplitude-of-vibration (msav) of the metal atom at temperature *T*. The **F** parameter can also be extracted from the U_{ij} values of the single crystal X-ray diffraction data, $\mathbf{F}_{X,T}$, and compared to the corresponding ME value, $\mathbf{F}_{M.T}$. This comparison is effected in Table 3, from which it is seen that for **1** at 100 K, $\mathbf{F}_{M,100} = 2.56$ whereas $\mathbf{F}_{X,100} = 3.87$. This large difference has been noted previously[46] for other organotin complexes, in contrast to iron organometallics, and may be related to the presence of relatively low frequency librational or torsional modes involving the tin atom in the covalent structure, or to the presence of static crystal imperfections to which the X-ray data are sensitive, but the ME data are not. In the present instance, the Sn atom is two-coordinate and ligated to the N atoms in the monomeric structure by two σ bonds of length 1.989 Å and bond angle 84.15(8)°. This configuration permits a large U_{ij} value in the X-ray data compared to the corresponding ME value. The relatively small resonance effect magnitude, as well as the rapid decrease of *f* with increasing temperature prevents the extension of the temperature-dependent ME data to higher values. The 147.9 K data show an effect magnitude of 0.37% and required accumulating 14.7×10^6 counts/channel for reasonable statistical accuracy.

Compound 2. Here, again, the ME spectra consist of a major and minor constituent, the area ratio at 90 K being ∼3.0:1. The hyperfine parameters are included in Table 3, from which it is noted that the IS in **2** is very much smaller than in **1**. In fact, the value of this parameter is close to that normally associated with Sn in the +4 oxidation state. However, given the determined stoichiometry of this compound, it is clear that the unusually small value of the IS must be associated with the ligation of the tin atom to the pentacarbonyl tungsten ligand, which effectively acts as an electron-withdrawing group.[47] The magnitude of the QS parameter in **2** is similar to that observed in other complexes in which the tin atom is ligated to a transition metal center (e.g., vide infra), and again a major contribution arises from the lone pair associated with the Sn center. The comparison of the $\mathbf{F}_X$ and $\mathbf{F}_M$ parameters at 100 K follows the same behavior as that noted for **1**, above. The origin of the minor tin resonance in the ME spectra of **2** has not been further elucidated.

Compound 3. For this compound, both the ^{119m}Sn and ^{57}Fe ME resonances have been determined over the temperature ranges $90 < T < 190$ and $90 < T < 248$ K, respectively. As noted above the ^{119}Sn spectra consist of a major and minor component with an area ratio of ∼2.1:1. The tin hyperfine parameters are included in Table 3 and are not otherwise remarkable, being consistent with a Sn(II) oxidation state of the metal atom. The examination of the **F** parameters at 100 K again shows that $\mathbf{F}_X > \mathbf{F}_M$ but the difference is only ∼13%; that is, much smaller than the corresponding differences noted for **1** and **2**. The most obvious rationalization of this fact is that in **3**, the tin atom, being coordinated to two iron centers as well as by the two nitrogen atoms of the 5-membered ring, is much more securely "tethered" and is less sensitive to the effects of the libration and torsional modes referred to above. The hyperfine parameters for the major component extracted from the ^{57}Fe ME spectra of **3** are included in Table 3 and a representative spectrum is shown in Supporting Information, Figure S2.

Here, again, there is evidence of a multiplicity of ^{57}Fe resonances, roughly in the ratio of 1:0.19:0.09 at 90 K. The three IS parameters are very similar, but the observed QS values range from 1.68 for the major resonance to 0.54 for the smallest. Because of the lower energy of the ^{57}Fe resonance compared to that of ^{119m}Sn, it is possible in this case to extend the ME measurements over a significantly longer range, and hence to determine the temperature dependencies of the IS and *f* parameters to better accuracy. The M_{eff} value[48] for the major constituent calculated from these data is ∼150 ± 15 Da, a value indicative of the strong covalent ligation of the Fe atom. In the present case it is interesting to note that $\mathbf{F}_{M,100}$ and $\mathbf{F}_{X,100}$ are nearly identical, as has been previously reported[45,49] for other organometallics in which the metal−ligand bonding involves largely π-orbitals of the transition metal, and where this group is well "tethered" to the remainder of the molecule.

Compound 5. Not surprisingly, the major Sn ME resonance hyperfine parameters observed for **5** are very similar to those noted for **1**, since the only significant difference between the two arises from the 5- versus 6-membered ring incorporating the metal atom (Figure 10). In this case, the minor resonance (∼5% of the total spectral area) has an IS close to 0 mm sec^{-1} and is most probably due to a minor contamination by Sn(IV) oxide. The major constituent hyperfine parameters are included in Table 3 and are not otherwise remarkable. The **F** values are $\mathbf{F}_{X,173} = 4.48$ and $\mathbf{F}_{M,173} = 3.74$, consistent with the earlier observations noted above. A comparison of the $\mathbf{F}_M$ values at various temperatures and their extrapolation to $T \rightarrow 0$, to the single crystal X-ray $\mathbf{F}_X$ value determined at 173 K is summarized graphically in Figure 10.

One further comment is appropriate with respect to **5**: because of the relatively "clean" nature of the ME spectra, it is observed that the area ratio of the two components of the QS doublet is

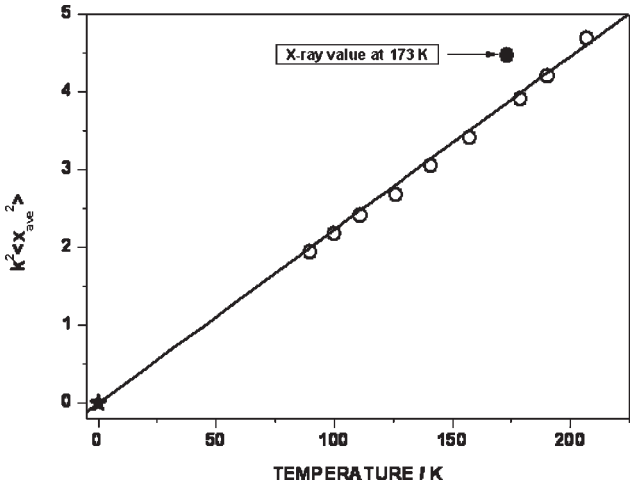

Figure 10. Parameter $k^2\langle x_{ave}^2\rangle$ for the ^{119}Sn Mössbauer resonance in **5**. The open data points refer to the ME data, the filled data point to that extracted from the single crystal X-ray data at 173 K, and the five-pointed star data point refers to the extrapolated value as $T \rightarrow 0$.

essentially temperature independent over the range $100 < T < 200$ K. Hence it is clear that there is no significant Gol'danskii–Karyagin effect[50] in the tin atom motion, and that the vibrational amplitudes are essentially isotropic over this temperature range, in agreement with the U_{ij} values reported at 173 K.

Compound 6. The ^{119}Sn ME spectra of this compound show only a single doublet, facilitating the subsequent data analysis. The IS value at 90 K (Table 3) is that associated with a tin atom ligated to a transition element, as noted above, indicating that there is a significant diminution in the s-electron density at Sn. The QS value at 90 K is particularly small, and this parameter is not at all sensitive to temperature. The $\mathbf{F}_{X,100}$ and $\mathbf{F}_{M,100}$ values are included in Table 3, and their ratio (1.55:1) is consistent with those reported earlier for these tin resonances, except that unusually the X-ray value is slightly smaller than the Mössbauer value. The area ratio of the two components of the QS doublet is temperature insensitive (1.08 ± 0.05 over the range $92 < T < 202$ K) again indicating isotropic motion of the tin atom in this solid. The Fe resonance in **6**, which could be acquired over only a limited temperature range ($90 < T < 150$ K), consists of the usual doublet, and the IS parameter is similar to that observed for **3**. On the other hand, the QS for this resonance is only about 25% of that observed for **3** reflecting the fact that the Fe atom in **6** is five-coordinate (and six-coordinate in **3**) reflecting the major crystallographic difference in the two iron sites. The agreement between the $\mathbf{F}_{x \text{ or } M}$ values at 100 K is satisfactory, given the limited temperature range over which data could be accumulated, and suggest that there are no major low-frequency librational or torsional modes influencing the iron atom motion in this compound.

EXPERIMENTAL SECTION

General Experimental Procedures. All air- and moisture-sensitive materials were weighed out, isolated, and stored in an argon-filled Saffron Beta glovebox. The solvents used were distilled HPLC grade and further dried and degassed using a commercially available solvent purification system (Anhydrous Engineering). Deuterated benzene was dried over potassium then vacuum transferred and kept over molecular sieves in the glovebox. Melting points were determined by sealing the sample in melting point tubes under argon in a glovebox prior to determination using a conventional apparatus. Elemental compositions (C, H, and N) were determined by sealing samples in airtight aluminum boats in a glovebox and were recorded on a Carlo Erba EA1108 CHN elemental analyzer. Solution NMR spectroscopy samples were prepared using dry and degassed deuterated solvent in airtight NMR tubes sealed with a Young's tap. ^{119}Sn spectra were run on Jeol Eclipse and Lambda 300 MHz spectrometers and referenced to an external sample of $SnMe_4$. ^{1}H and ^{13}C NMR spectra were run on Jeol Eclipse 300 and Lambda 300 MHz spectrometers and were referenced to the internal solvent peaks. DOSY experiments were performed using a Varian 500 MHz spectrometer at 25.0 °C using peak integrations to give diffusion coefficients.

Temperature-dependent Mössbauer spectra were acquired in transmission geometry by using both the ^{57}Fe and the ^{119m}Sn resonances. The former was collected using a ~50 mCi source of ^{57}Co in a Rh matrix, and all iron isomer shifts are referred to the center of a room temperature α-Fe absorption spectrum which was also used for spectrometer calibration. The latter were collected using a 2 mCi $^{119\,m}$Sn source in a $BaSnO_3$ matrix, and all tin isomer shifts are referenced to a room temperature $BaSnO_3$ absorber spectrum. Temperatures were monitored using the Daswin program, and are considered stable to ±0.2 K over the data acquisition intervals.

The Mössbauer samples were transferred from sealed Pyrex tubes to O-ring equipped Perspex sample holders in a glovebox, and immediately cooled to liquid nitrogen temperature prior to spectroscopic examination. To ascertain that there was no sample loss during the extended data collection intervals (crucial for the data interpretation related to the m. sav values) the transmission rate through the sample was monitored both before and after each temperature run.

Stannylenes **1** and **5** were synthesized as reported previously.[18d] A racemic mixture of the chiral diamine **10**[44a] and $[(Ph_3P)_2Pt(C_2H_4)]$[51] were synthesized as previously described. Despite repeated attempts, satisfactory elemental analyses for a number of the products could not be obtained. This is presumably due to the range of different products isolated from some of the reactions and the high air- and moisture-sensitivity of the compounds.

*$[(CO)_5W{-}Sn\{N(Dipp)CH_2\}_2]$ (**2**).* A solution of $W(CO)_6$ (0.257 g, 0.73 mmol) dissolved in thf (20 cm^3) was irradiated with a UV lamp for 2 h forming a clear yellow solution indicative of $[W(CO)_5(thf)]$. A solution of $[Sn\{N(Dipp)CH_2\}_2]$ (**1**) (0.363 g, 0.73 mmol) in thf (10 cm^3) was then added, and the reaction mixture was stirred overnight. All of the solvent was removed from the red/orange solution, and the solid was extracted into *n*-hexane (30 cm^3) and filtered (porosity 3 sinter with Celite). The red solution was reduced in volume in vacuo and placed at −20 °C for 1 week upon which red/purple crystals were observed (0.220 g, 0.268 mmol, 37%).

^{1}H NMR (300 MHz, 25 °C, C_6D_6): δ (ppm) 7.13−7.11 (m, Ar H), 3.81 (s with unresolved ^{119}Sn and ^{117}Sn satellites $^3J(^1H{-}Sn) \approx 22$ Hz, CH_2), 3.62 (septet $^3J(^1H{-}^1H) = 6.97$ Hz, Dipp CH), 1.35 (d $^3J(^1H{-}^1H) = 6.97$ Hz, Dipp Me), 1.28 (d $^3J(^1H{-}^1H) = 6.97$ Hz, Dipp Me). **^{13}C NMR (75.5 MHz, 25 °C, C_6D_6):** δ (ppm) 197.7 (*trans* W-CO), 194.4 (*cis* W-CO), 146.8 (*ortho* Ar C), 144.1 (*ipso* Ar C), 127.3 (*para* Ar C), 124.4 (*meta* Ar C), 60.6 (CH_2), 29.2, 26.0, 24.8 (^{i}Pr carbons). **^{119}Sn NMR (112 MHz, 25 °C, C_6D_6):** δ (ppm) 426.2 (s with ^{183}W satellites $^1J(^{119}Sn{-}^{183}W) = 1150$ Hz). **IR (*n*-hexane):** ν(cm^{-1}) 2076.2 (CO stretch), 1960.4 (CO stretch), 1928.7 (shoulder, CO stretch). **Elemental Analysis:** Calculated (%): C 45.34, H 4.66, N 3.41. Found (%): C 45.60, H 4.99, N 3.54.

*$[(CO)_4Fe(\mu\text{-}Sn\{N(Dipp)CH_2\}_2)]_2$ (**3**).* To a suspension of $[Fe_2(CO)_9]$ (144 mg, 0.40 mmol) in toluene (10 mL) was added a solution of $[Sn\{N(Dipp)CH_2\}_2]$ (**1**) (197 mg, 0.40 mmol) in toluene (10 mL), and the mixture was stirred overnight. A clear, dark red solution was observed, and all the solvent and any $[Fe(CO)_5]$ produced was removed under vacuum. The solid was extracted with toluene (30 mL) and filtered (porosity 3 sinter with Celite) giving a clear dark red solution which was

dx.doi.org/10.1021/ic101920x |*Inorg. Chem.* 2011, 50, 2252–2263

Table 4. Selected Crystallographic and Data Collection Parameters for Compounds 2−4, 6−8, and 10−12

	2	3	4	6	7
color, habit	red prism	red prism	red block	yellow plate	red block
size/mm	0.11 × 0.10 × 0.02	0.13 × 0.08 × 0.05	0.20 × 0.13 × 0.10	0.20 × 0.12 × 0.03	0.21 × 0.14 × 0.04
empirical formula	$C_{31}H_{38}N_2O_5SnW$	$C_{60}H_{76}Fe_2N_4O_8Sn_2$	$C_{34}H_{38}Fe_2N_2O_8Sn$	$C_{34.5}H_{44}FeN_2O_4Sn$	$C_{35}H_{40}Fe_2N_2O_8Sn$
M	821.19	1330.32	833.05	725.26	847.08
crystal system	orthorhombic	monoclinic	monoclinic	monoclinic	triclinic
space group	*Pnma*	$P2_1/n$	$P2_1/m$	$P2_1$	$P\bar{1}$
a/Å	16.6243(3)	13.4655(16)	9.7677(3)	9.7070(4)	17.6709(5)
b/Å	18.9240(7)	11.7855(13)	18.7855(6)	36.8631(15)	21.4182(6)
c/Å	10.4192(2)	19.163(2)	10.3823(3)	9.7894(4)	22.3233(6)
α/deg	90	90	90	90	61.7630(10)
β/deg	90	102.069(2)	112.1130(10)	101.050(2)	89.7080(10)
γ/deg	90	90	90	90	81.8280(10)
V/Å^3	3277.86(15)	2973.9(6)	1764.93(9)	3438.0(2)	7349.1(4)
Z	4	2	2	4	8
μ/mm^{-1}	4.307	1.364	1.564	1.186	1.504
T/K	100	100	100	100	100
$\theta_{min,max}$	2.55,32.87	1.69,27.50	2.12, 27.48	3.47,33.13	1.04,27.48
completeness to θ_{max}	0.941	0.997	1.000	0.995	0.997
reflections: total/independent	36025/5899	25856/6822	27016/4176	38795/19511	152337/33588
R_{int}	0.0507	0.0595	0.0388	0.0692	0.0419
final $R1$ ($I > 2\sigma$) and $wR2$ (all data)	0.0285, 0.0542	0.0404, 0.1015	0.0300, 0.0837	0.0576, 0.1102	0.0319, 0.0788
largest peak, hole/e Å^{-3}	0.859, −1.543	1.226, −0.630	1.416, −1.072	1.420, −1.764	0.907, −0.603
ρ_{calc}/g cm^{-3}	1.664	1.486	1.568	1.401	1.531
Flack parameter	n/a	n/a	n/a	0.36(2)	n/a

	8	10	11	12
color, habit	red prism	yellow rod	yellow block	orange rod
size/mm	0.40 × 0.20 × 0.05	0.30 × 0.08 × 0.08	0.19 × 0.06 × 0.04	0.40 × 0.11 × 0.11
empirical formula	$C_{112}H_{130}N_4P_2Pt_2Sn_2$	$C_{12}H_{26}N_2Sn$	$C_{16}H_{26}FeN_2O_4Sn$	$C_{19}H_{31}MnN_2O_2Sn$
M	2221.70	317.06	484.93	493.09
crystal system	monoclinic	monoclinic	monoclinic	monoclinic
space group	$C2/c$	$P2_1/c$	$C2/c$	$P2_1/c$
a/Å	19.8884(6)	23.3287(6)	17.9372(6)	6.6047(8)
b/Å	26.9543(8)	6.4072(2)	9.8950(3)	17.932(2)
c/Å	19.0243(6)	21.6934(5)	12.1219(5)	17.704(2)
α/deg	90	90	90	90
β/deg	92.934(2)	117.6900(10)	111.787(2)	94.222(2)
γ/deg	90	90	90	90
V/Å^3	10185.1(5)	2871.19(13)	1997.82(12)	2091.2(4)
Z	4	8	4	4
μ/mm^{-1}	3.302	1.756	1.996	1.812
T/K	100	100	100	100
$\theta_{min,max}$	1.27,28.35	1.75,28.27	3.26,27.53	2.31,27.51
completeness to θ_{max}	0.996	0.997	0.995	0.998
reflections: total/independent	75254/12690	65157/7120	9783/2291	18763/4801
R_{int}	0.0527	0.0457	0.0237	0.0276
final $R1$ ($I > 2\sigma$) and $wR2$ (all data)	0.0243, 0.0721	0.0367, 0.0927	0.0195, 0.0518	0.0264, 0.0874
largest peak, hole/e Å^{-3}	0.731, −0.756	4.861, −1.070	1.128, −0.518	0.616, −1.251
ρ_{calc}/g cm^{-3}	1.449	1.467	1.612	1.566
Flack parameter	n/a	n/a	n/a	n/a

reduced in vacuo and placed at −20 °C for 3 days upon which red crystals were observed (89 mg, 0.067 mmol, 33% yield).

^{1}H NMR (300 MHz, 25 °C, C_6D_6): δ (ppm) 7.13−7.00 (m, Ar H), 3.75 (s with unresolved ^{119}Sn and ^{117}Sn satellites $^3J(^1H-Sn) \approx 27$ Hz, CH_2), 3.63 (septet $^3J(^1H-^1H) = 6.97$ Hz, Dipp CH), 1.30 (d $^3J(^1H-^1H) = 6.97$ Hz, Dipp Me), 1.27 (d $^3J(^1H-^1H) = 6.97$ Hz, Dipp Me). **^{13}C NMR (75.5 MHz, 25 °C, C_6D_6)**: δ (ppm) 212.6 (Fe-CO), 146.4 (*ortho* Ar C), 143.9 (*ipso* Ar C), 126.8 (*para* Ar C), 124.0 (*meta* Ar C),

dx.doi.org/10.1021/ic101920x |*Inorg. Chem.* 2011, 50, 2252–2263

59.6 (CH_2), 28.7, 24.8, 24.8 (^{i}Pr carbons). **^{119}Sn NMR (112 MHz, 25 °C, C_6D_6):** δ (ppm) 525.3 (s). **IR (*n*-hexane):** ν(cm^{-1}) 2091.8 (m, CO stretch), 2039.9 (s, CO stretch), 2014.6 (s, CO stretch), 1962.2 (m, CO stretch). **IR (nujol mull):** ν(cm^{-1}) 2092.7 (w), 2046.1 (s), 2008.9 (s), 1995.2 (s). **m.p.:** Decomposed above 205 °C.

*[(CO)$_4$Fe−Sn{N(Dipp)CH$_2$}$_2$CH$_2$] (**6**).* To a suspension of [$Fe_2(CO)_9$] (151 mg, 0.41 mmol) in toluene (10 mL) was added a solution of [Sn{N(Dipp)CH$_2$}$_2$CH$_2$] (**5**) (212 mg, 0.41 mmol) in toluene (10 mL), and the mixture was stirred overnight. A dark orange/red solution was observed, and all the solvent and any [$Fe(CO)_5$] produced was removed under vacuum. The solid was extracted with hexane (30 mL) and filtered (porosity 3 sinter with Celite) giving a clear orange/red solution which was reduced in vacuo and placed at −20 °C overnight upon which yellow crystals were observed (123 mg, 0.18 mmol, 44% yield).

^{1}H NMR (300 MHz, 25 °C, C_6D_6): δ (ppm) 7.14−7.09 (m, Ar H), 3.61 (septet $^3J(^1H-^1H)$ = 6.96 Hz, Dipp CH), 3.38 (t $^3J(^1H-^1H)$ = 4.95 Hz, N−CH_2), 2.10 (m, CH_2) 1.35 (d $^3J(^1H-^1H)$ = 6.96 Hz, Dipp Me), 1.27 (d $^3J(^1H-^1H)$ = 6.96 Hz, Dipp Me). **^{13}C NMR (75.5 MHz, 25 °C, C_6D_6):** δ (ppm) 212.5 (Fe-CO), 146.9 (*ortho* Ar C), 144.8 (*ipso* Ar C), 127.4 (*para* Ar C), 124.3 (*meta* Ar C), 58.4 (N−CH_2), 35.2 (CH_2), 28.4, 25.4, 24.9 (^{i}Pr carbons). **^{119}Sn NMR (112 MHz, 25 °C, C_6D_6):** δ (ppm) 498.0 (s). **IR (*n*-hexane):** ν(cm^{-1}) 2061.5 (m), 2052.1 (m), 1990.2 (s), 1970.0 (s). **IR (nujol mull):** ν(cm^{-1}) 2089.8 (w), 2059.7 (w sh.), 2042.9 (s), 2021.4 (w sh.), 1966.9 (s sh.), 1940.7 (s). **m.p.:** 164−168 °C. Decomposed above 178 °C.

*[(Ph$_3$P)Pt(μ-Sn{N(Dipp)CH$_2$}$_2$)]$_2$ (**8**).* [$(Ph_3P)_2Pt(C_2H_4)$] (150 mg, 0.20 mmol) and [Sn{N(Dipp)CH$_2$}$_2$] (**1**) (100 mg, 0.20 mmol) were dissolved in C_6D_6 (1.0 cm^3) giving a deep red solution which was transferred to an NMR tube equipped with a Young's tap. Upon standing for a week, the sample crystallized as bright red crystals suitable for X-ray analysis.

^{1}H NMR (300 MHz, 25 °C, C_6D_6): δ (ppm) 7.42 (d J = 7.14 Hz, 8 H, Ar H), 7.23 (m, Ar H), 7.02−6.90 (m 12 H, Ar H), 3.97 (br. s, 4 H, CH_2), 3.81 (septet $^3J(^1H-^1H)$ = 6.96 Hz, 4 H, Dipp CH), 1.35 (d $^3J(^1H-^1H)$ = 6.96 Hz, 12 H, Dipp Me), 1.13 (d $^3J(^1H-^1H)$ = 6.96 Hz, 12 H, Dipp Me). **^{1}H NMR (300 MHz, 60 °C, C_6D_6):** δ (ppm) spectrum identical to that at room temperature. **^{31}P{^{1}H} NMR (121.4 MHz, 25 °C, C_6D_6):** δ(ppm) 52.0 (br. s with broad ^{195}Pt satellites $^1J(^{31}P-^{195}Pt)$ = 5173 Hz). **^{31}P{^{1}H} NMR (121.4 MHz, 60 °C, C_6D_6):** δ(ppm) 52.8 (br. s with broad ^{195}Pt satellites $^1J(^{31}P-^{195}Pt)$ = 5215 Hz). **^{119}Sn NMR (112 MHz, 25 °C, C_6D_6):** δ (ppm) extremely broad signal at about 500.

*rac-[Sn{N(^{t}Bu)CHMe}$_2$] (**10**).* ^{n}BuLi (5.2 mL 1.6 M solution in hexane, 8.42 mmol) was added to a solution of {HN(^{t}Bu)CHMe}$_2$ (**9**) (0.838 g, 4.2 mmol) in Et_2O (40 mL), and the clear colorless solution was stirred for 2 h. This solution was then transferred slowly by cannula to a −78 °C suspension of $SnCl_2$ (0.793 g, 4.2 mmol) in Et_2O (20 mL), and the cloudy orange solution was allowed to warm to room temperature and stir overnight. The solvent was removed under reduced pressure, and the solid was extracted with *n*-hexane (60 mL) and filtered (porosity 3 sinter with Celite). The bright yellow solution was reduced in volume in vacuo and then placed at −20 °C overnight upon which yellow crystals were observed. (0.818 g, 2.58 mmol, 61% yield). The product sublimes at 5 × 10^{-1} Torr and 100 °C, and displays thermochromic behavior as frozen solutions of the stannylene in *n*-hexane at −196 °C are bright red.

^{1}H NMR (300 MHz, 25 °C, C_6D_6): δ (ppm) 3.32 (q $^3J(^1H-^1H)$ = 6.23 Hz, CH), 1.25 (s, *tert*-butyl), 1.20 (d, $^3J(^1H-^1H)$ = 6.23 Hz, Me). **^{13}C NMR (75.5 MHz, 25 °C, C_6D_6):** δ (ppm) 64.3 (NCH), 55.9 (NC(CH_3)$_3$), 34.0 (C(CH_3)$_3$), 28.5 (CHCH_3). **^{119}Sn NMR (112 MHz, 25 °C, C_6D_6):** δ (ppm) 454. **Elemental Analysis:** Calculated (%): C 45.46, H 8.27, N 8.84. Found (%): C 45.33, H 8.77, N 8.50. **m.p.:** 172−177 °C. Decomposed above 210 °C.

*rac-[(CO)$_4$Fe−Sn{N(^{t}Bu)CHMe}$_2$] (**11**).* To a suspension of [$Fe_2(CO)_9$] (172 mg, 0.47 mmol) in toluene (10 mL) was added a solution of *rac*-[Sn{N(^{t}Bu)CHMe}$_2$] (**10**) (150 mg, 0.47 mmol) in toluene (10 mL), and the mixture was stirred overnight. A dark orange/red solution was observed, and all the solvent and any [$Fe(CO)_5$] produced was removed under vacuum. The solid was extracted with hexane (20 mL) and filtered (porosity 3 sinter with Celite) giving a clear red solution which was reduced in vacuo and placed at −20 °C for 3 days upon which orange/red crystals were observed (98 mg, 0.20 mmol, 43% yield).

^{1}H NMR (300 MHz, 25 °C, C_6D_6): δ (ppm) 3.03 (q $^3J(^1H-^1H)$ = 6.04 Hz with unresolved ^{119}Sn and ^{117}Sn satellites $^3J(^1H-Sn) \approx 36$ Hz, CH), 1.15 (s, *tert*-butyl), 0.96 (d, $^3J(^1H-^1H)$ = 6.04 Hz, Me). **^{13}C NMR (75.5 MHz, 25 °C, C_6D_6):** δ (ppm) 214.2 (Fe-CO), 61.6 (NCH), 56.8 (NC(CH_3)$_3$), 33.4 (C(CH_3)$_3$), 27.3 (CHCH_3). **^{119}Sn NMR (112 MHz, 25 °C, C_6D_6):** δ (ppm) 534.0. **IR (*n*-hexane):** ν(cm^{-1}) 2034.0 (s), 1963.9 (m), 1934.4 (s), 1907.2 (s). **m.p.:** 70−73 °C. Decomposed above 119 °C.

*rac-[Cp(CO)$_2$Mn−Sn{N(^{t}Bu)CHMe}$_2$] (**12**).* A solution of [CpMn(CO)$_3$] (100 mg, 0.49 mmol) dissolved in thf (20 cm^3) was irradiated with a UV lamp for 2 h forming a deep red/purple solution. A solution of *rac*-[Sn{N(^{t}Bu)CHMe}$_2$] (**10**) (155 mg, 0.49 mmol) in thf (10 cm^3) was then added, and the reaction mixture was stirred overnight. All of the solvent was removed from the clear orange solution, and the solid was extracted into *n*-hexane (20 cm^3) and filtered (porosity 3 sinter with Celite). The bright orange solution was reduced in volume in vacuo and placed at −20 °C, and the product was formed as yellow crystals in two crops (56 mg, 0.114 mmol, 23%).

^{1}H NMR (300 MHz, 25 °C, C_6D_6): δ (ppm) 4.04 (s with broad satellites ≈12 Hz, Cp), 3.21 (q $^3J(^1H-^1H)$ = 6.23 Hz, CH), 1.29 (s, *tert*-butyl), 1.10 (d, $^3J(^1H-^1H)$ = 6.23 Hz, Me). **^{13}C NMR (75.5 MHz, 25 °C, C_6D_6):** δ (ppm) 231.1 (s, weak, Mn-CO), 230.6 (s, weak, Mn-CO), 78.2 (Cp), 62.3 (NCH), 56.2 (NC(CH_3)$_3$), 34.0 (C(CH_3)$_3$), 28.9 (CHCH_3). **^{119}Sn NMR (112 MHz, 25 °C, C_6D_6):** δ (ppm) 625 (broad). **IR (*n*-hexane):** ν(cm^{-1}) 1921.6 (s), 1855.4 (s). **m.p.:** 120−126 °C. Decomposed above 144 °C.

X-ray Crystallography. Crystals suitable for X-ray diffraction analysis of **2**−**4**, **6**−**8**, **10**−**12** were grown as described above, mounted in an inert oil and then transferred to the cold gas stream of the diffractometer. Experiments were made with a Bruker-AXS Kappa-APEX-II four circle diffractometer[52] employing Mo-Kα radiation (λ = 0.71073 Å), except **2** where a Oxford diffraction Gemini four-circle diffractometer employing Mo-Kα radiation (λ = 0.71073 Å) was used. Intensities were integrated from several series of exposures, and absorption corrections were applied based on multiple- and symmetry-equivalent measurements.[53] Structures were solved by direct methods and refined by least-squares on weighted F^2 values for all reflections.[54] All non-hydrogen atoms were assigned anisotropic displacement parameters and refined without positional constraints. Hydrogen atoms were constrained to ideal geometries and refined with fixed isotropic displacement parameters. Refinement proceeded smoothly to give the residuals shown in Table 4. Complex neutral-atom scattering factors were used.[55] Crystals of **10** were twinned, and the twin law [−1 0 −1 0 −1 0 0 0 1] was used with the BASF refining to 0.49.

CCDC reference numbers 807655 (**2**), 807656 (**3**), 807657 (**4**), 807658 (**6**), 807659 (**7**), 807660 (**8**), 807661 (**10**), 807662 (**11**), and 807663 (**12**).

CONCLUSIONS

In summary we have shown that *N*-heterocyclic stannylenes are competent ligands toward a range of different transition metals (W, Fe, Pt, and Mn). The binding of NHSns to metals structurally has only minimal effect on the NHSn. Interestingly, whereas NHSns will bind in a terminal manner to transition metal centers, they also show a distinct propensity to adopt a bridging position across dinuclear metal units. The balance between terminal and bridging positions for the stannylene is evidently closely balanced as shown by the observations of both monomers and dimers for the same molecular unit in both solid

state and in solution. ^{119}Sn and ^{57}Fe Mössbauer spectroscopy of the complexes showed significant changes to the environment around the Sn centers upon coordination to transition metals.

■ ASSOCIATED CONTENT

Supporting Information. Mössbauer spectra of **1** and **3**. Crystallographic data in CIF format. This material is available free of charge via the Internet at http://pubs.acs.org.

■ AUTHOR INFORMATION

Corresponding Author

*E-mail: herber@vms.huji.ac.il (R.H.H.), chris.russell@bris.ac.uk (C.A.R.). Fax: +972 (0)2 658 6347 (R.H.H.), +44 (0)117 925 1295 (C.A.R.). Phone: +972 (0)2 658 4244 (R.H.H.), +44 (0)117 928 7599 (C.A.R.).

■ ACKNOWLEDGMENT

We acknowledge Dr. Craig Butts (Bristol) for help with DOSY experiments and Dr. Natalie Fey (Bristol) for advice on this manuscript. S.M.M. would like to thank the University of Bristol for funding. We are also indebted to David Mocatta for the careful glovebox transfer of the many air/moisture sensitive samples to the ME sample holders prior to spectroscopic examination.

■ REFERENCES

(1) (a) Bourissou, D.; Guerret, O.; Gabbaï, F. P.; Bertrand, G. *Chem. Rev.* **2000**, *100*, 39. (b) Hahn, F. E. *Angew. Chem., Int. Ed.* **2006**, *45*, 1348. (c) Hahn, F. E.; Jahnke, M. C. *Angew. Chem., Int. Ed.* **2008**, *47*, 3122.

(2) Arduengo, A. J.; Harlow, R. L.; Kline, M. *J. Am. Chem. Soc.* **1991**, *113*, 361.

(3) (a) Herrmann, W. A.; Köcher, C. *Angew. Chem., Int. Ed. Engl.* **1997**, *36*, 2163. (b) Herrmann, W. A. *Angew. Chem., Int. Ed.* **2002**, *41*, 1290. (c) Crudden, C. M.; Allen, D. P. *Coord. Chem. Rev.* **2004**, *248*, 2247. (d) Grubbs, R. H. *Tetrahedron* **2004**, *60*, 7117. (e) Diez-Gonzalez, S.; Marion, N.; Nolan, S. P. *Chem. Rev.* **2009**, *109*, 3612.

(4) (a) Wang, Y. Z.; Xie, Y. M.; Wei, P. R.; King, R. B.; Schaefer, H. F.; Schleyer, P. V.; Robinson, G. H. *Science* **2008**, *321*, 1069. (b) Wang, Y.; Robinson, G. H. *Chem. Commun* **2009**, 5201. (c) Wolf, R.; Uhl, W. *Angew. Chem., Int. Ed.* **2009**, *48*, 6774.

(5) Kühl, O. *Coord. Chem. Rev.* **2009**, *253*, 2481.

(6) (a) Arduengo, A. J.; Goerlich, J. R.; Marshall, W. J. *J. Am. Chem. Soc.* **1995**, *117*, 11027. (b) Alder, R. W.; Blake, M. E.; Bortolotti, C.; Bufali, S.; Butts, C. P.; Linehan, E.; Oliva, J. M.; Orpen, A. G.; Quayle, M. J. *Chem. Commun.* **1999**, 241. (c) Alder, R. W.; Blake, M. E.; Chaker, L.; Harvey, J. N.; Paolini, F.; Schütz, J. *Angew. Chem., Int. Ed.* **2004**, *43*, 5896. (d) Binobaid, A.; Iglesias, M.; Beetstra, D. J.; Kariuki, B.; Dervisi, A.; Fallis, I. A.; Cavell, K. J. *Dalton Trans.* **2009**, 7099.

(7) Cesar, V.; Bellemin-Laponnaz, S.; Gade, L. H. *Chem. Soc. Rev.* **2004**, *33*, 619.

(8) (a) Lavallo, V.; Mafhouz, J.; Canac, Y.; Donnadieu, B.; Schoeller, W. W.; Bertrand, G. *J. Am. Chem. Soc.* **2004**, *126*, 8670. (b) Frey, G. D.; Lavallo, V.; Donnadieu, B.; Schoeller, W. W.; Bertrand, G. *Science* **2007**, *316*, 439.

(9) Martin, D.; Baceiredo, A.; Gornitzka, H.; Schoeller, W. W.; Bertrand, G. *Angew. Chem., Int. Ed.* **2005**, *44*, 1700.

(10) Mizuhata, Y.; Sasamori, T.; Tokitoh, N. *Chem. Rev.* **2010**, *110*, 3850.

(11) (a) Hill, M. S.; Hitchcock, P. B. *Chem. Commun.* **2004**, 1818. (b) Baker, R. J.; Jones, C. *Coord. Chem. Rev.* **2005**, *249*, 1857. (c) Jones, C.; Junk, P. C.; Platts, J. A.; Stasch, A. *J. Am. Chem. Soc.* **2006**, *128*, 2206.

(12) (a) Carmalt, C. J.; Lomeli, V.; McBurnett, B. G.; Cowley, A. H. *Chem. Commun* **1997**, 2095. (b) Gudat, D.; Gans-Eichler, T.; Nieger, M. *Chem. Commun.* **2004**, 2434.

(13) (a) Dutton, J. L.; Tuononen, H. M.; Jennings, M. C.; Ragogna, P. J. *J. Am. Chem. Soc.* **2006**, *128*, 12624. (b) Tuononen, H. M.; Roesler, R.; Duffon, J. L.; Ragogna, P. J. *Inorg. Chem.* **2007**, *46*, 10693.

(14) Mizuhata, Y.; Sasamori, T.; Tokitoh, N. *Chem. Rev.* **2009**, *109*, 3479.

(15) (a) Davidson, P. J.; Lappert, M. F. *J. Chem. Soc., Chem. Commun.* **1973**, 317. (b) Davidson, P. J.; Lappert, M. F.; Pearce, R. *Acc. Chem. Res.* **1974**, *7*, 209. (c) Davidson, P. J.; Lappert, M. F.; Pearce, R. *Chem. Rev.* **1976**, *76*, 219.

(16) (a) Denk, M.; Lennon, R.; Hayashi, R.; West, R.; Belyakov, A. V.; Verne, H. P.; Haaland, A.; Wagner, M.; Metzler, N. *J. Am. Chem. Soc.* **1994**, *116*, 2691. (b) Gehrhus, B.; Lappert, M. F.; Heinicke, J.; Boese, R.; Blaser, D. *J. Chem. Soc., Chem. Commun.* **1995**, 1931. (c) Gehrhus, B.; Hitchcock, P. B.; Lappert, M. F.; Heinicke, J.; Boese, R.; Blaser, D. *J. Organomet. Chem.* **1996**, *521*, 211. (d) Haaf, M.; Schmiedl, A.; Schmedake, T. A.; Powell, D. R.; Millevolte, A. J.; Denk, M.; West, R. *J. Am. Chem. Soc.* **1998**, *120*, 12714. (e) Heinicke, J.; Oprea, A.; Kindermann, M. K.; Karpati, T.; Nyulaszi, L.; Veszpremi, T. *Chem.—Eur. J.* **1998**, *4*, 541. (f) Haaf, M.; Schmedake, T. A.; West, R. *Acc. Chem. Res.* **2000**, *33*, 704. (g) Driess, M.; Yao, S. L.; Brym, M.; van Wüllen, C.; Lentz, D. *J. Am. Chem. Soc.* **2006**, *128*, 9628. (h) Tomasik, A. C.; Mitra, A.; West, R. *Organometallics* **2009**, *28*, 378.

(17) (a) Herrmann, W. A.; Denk, M.; Behm, J.; Scherer, W.; Klingan, F. R.; Bock, H.; Solouki, B.; Wagner, M. *Angew. Chem., Int. Ed. Engl.* **1992**, *31*, 1485. (b) Kühl, O. *Coord. Chem. Rev.* **2004**, *248*, 411. (c) Driess, M.; Yao, S. L.; Brym, M.; van Wüllen, C. *Angew. Chem., Int. Ed.* **2006**, *45*, 4349. (d) Gans-Eichler, T.; Gudat, D.; Nattinen, K.; Nieger, M. *Chem.—Eur. J.* **2006**, *12*, 1162. (e) Zabula, A. V.; Hahn, E. *Eur. J. Inorg. Chem.* **2008**, 5165. (f) Tomasik, A. C.; Hill, N. J.; West, R. *J. Organomet. Chem.* **2009**, *694*, 2122.

(18) (a) Veith, M. *Angew. Chem., Int. Ed. Engl.* **1975**, *14*, 263. (b) Gans-Eichler, T.; Gudat, D.; Nieger, M. *Angew. Chem., Int. Ed.* **2002**, *41*, 1888. (c) Charmant, J. P. H.; Haddow, M. F.; Hahn, E.; Heitmann, D.; Fröhlich, R.; Mansell, S. M.; Russell, C. A.; Wass, D. F. *Dalton Trans.* **2008**, 6055. (d) Mansell, S. M.; Russell, C. A.; Wass, D. F. *Inorg. Chem.* **2008**, *47*, 11367.

(19) Jacobsen, H.; Correa, A.; Poater, A.; Costabile, C.; Cavallo, L. *Coord. Chem. Rev.* **2009**, *253*, 687; *Coord. Chem. Rev.* **2009**, *253*, 2784.

(20) Arnold, P. L.; Pearson, S. *Coord. Chem. Rev.* **2007**, *251*, 596.

(21) From a search of the Cambridge Structural Database, Version 5.30, update 3.

(22) (a) Garrison, J. C.; Simons, R. S.; Kofron, W. G.; Tessier, C. A.; Youngs, W. J. *Chem. Commun.* **2001**, 1780. (b) Gischig, S.; Togni, A. *Organometallics* **2005**, *24*, 203.

(23) (a) Petz, W. *Chem. Rev.* **1986**, *86*, 1019. (b) Lappert, M. F.; Rowe, R. S. *Coord. Chem. Rev.* **1990**, *100*, 267.

(24) (a) Furstner, A.; Krause, H.; Lehmann, C. W. *Chem. Commun.* **2001**, 2372. (b) Herrmann, W. A.; Harter, P.; Gstottmayr, C. W. K.; Bielert, F.; Seeboth, N.; Sirsch, P. *J. Organomet. Chem.* **2002**, *649*, 141.

(25) Waterman, R.; Hayes, P. G.; Tilley, T. D. *Acc. Chem. Res.* **2007**, *40*, 712.

(26) (a) Veith, M.; Stahl, L. *Angew. Chem., Int. Ed. Engl.* **1993**, *32*, 106. (b) Veith, M.; Müller, A.; Stahl, L.; Nötzel, M.; Jarczyk, M.; Huch, V. *Inorg. Chem.* **1996**, *35*, 3848. (c) Bazinet, P.; Yap, G. P. A.; Richeson, D. S. *J. Am. Chem. Soc.* **2001**, *123*, 11162. (d) Kühl, O.; Lönnecke, P.; Heinicke, J. *Inorg. Chem.* **2003**, *42*, 2836. (e) Ullah, F.; Kühl, O.; Baior, G.; Veszpremi, T.; Jones, P. G.; Heinicke, J. *Eur. J. Inorg. Chem.* **2009**, 221.

(27) Veith, M.; Stahl, L.; Huch, V. *Chem. Commun.* **1990**, 359.

(28) Veith, M. *Angew. Chem., Int. Ed. Engl.* **1987**, *26*, 1.

(29) Zabula, A. V.; Pape, T.; Hepp, A.; Hahn, F. E. *Organometallics* **2008**, *27*, 2756.

(30) Zabula, A. V.; Pape, T.; Hepp, A.; Hahn, F. E. *Dalton Trans.* **2008**, 5886.

(31) Hahn, F. E.; Zabula, A. V.; Pape, T.; Hepp, A.; Tonner, R.; Haunschild, R.; Frenking, G. *Chem.—Eur. J.* **2008**, *14*, 10716.

(32) Diez-Gonzalez, S.; Stevens, E. D.; Scott, N. M.; Petersen, J. L.; Nolan, S. P. *Chem.—Eur. J.* **2008**, *14*, 158.

(33) Hill, A. F. *Organotransition Metal Chemistry*; Royal Society of Chemistry: Cambridge, U.K., 2002.
(34) Lappert, M. F.; Power, P. P. *J. Chem. Soc., Dalton Trans.* **1985**, 51.
(35) A search of the Cambridge Structural Database, version 5.30, update 3 gave 244 independent distances.
(36) Hitchcock, P. B.; Lappert, M. F.; Thomas, S. A.; Thorne, A. J.; Carty, A. J.; Taylor, N. J. *J. Organomet. Chem.* **1986**, *315*, 27.
(37) Schneider, J. J.; Czap, N.; Blaser, D.; Boese, R.; Ensling, J.; Gutlich, P.; Janiak, C. *Chem.—Eur. J.* **2000**, *6*, 468.
(38) Schneider, J. J.; Czap, N.; Blaser, D.; Boese, R. *J. Am. Chem. Soc.* **1999**, *121*, 1409; Schneider, J. J.; Czap, N.; Blaser, D.; Boese, R. *J. Am. Chem. Soc.* **1999**, *121*, 10856.
(39) (a) Dixon, J. A.; Schiessler, R. W. *J. Phys. Chem.* **1954**, *58*, 430. (b) Lide, D. R. *CRC Handbook of Chemistry and Physics*; CRC Press: Boca Raton, FL, 1995.
(40) Mastrorilli, P. *Eur. J. Inorg. Chem.* **2008**, 4835.
(41) (a) Bushnell, G. W.; Eadie, D. T.; Pidcock, A.; Sam, A. R.; Holmessmith, R. D.; Stobart, S. R.; Brennan, E. T.; Cameron, T. S. *J. Am. Chem. Soc.* **1982**, *104*, 5837. (b) Campbell, G. K.; Hitchcock, P. B.; Lappert, M. F.; Misra, M. C. *J. Organomet. Chem.* **1985**, *289*, C1.
(42) (a) Veith, M. *Z. Naturforsch.* **1978**, *33*, 1. (b) Hahn, F. E.; Wittenbecher, L.; Kuhn, M.; Lugger, T.; Frohlich, R. *J. Organomet. Chem.* **2001**, *617*, 629. (c) Hahn, F. E.; Wittenbecher, L.; Le Van, D.; Zabula, A. V. *Inorg. Chem.* **2007**, *46*, 7662. (d) Zabula, A. V.; Pape, T.; Hepp, A.; Schappacher, F. M.; Rodewald, U. C.; Pottgen, R.; Hahn, F. E. *J. Am. Chem. Soc.* **2008**, *130*, 5648.
(43) During revision of this manuscript, an example of a chiral *N*-heterocyclic stannylene was published. See: Dickschat, J. V.; Urban, S.; Pape, T.; Glorius, F.; Hahn, F. E. *Dalton Trans.* **2010**, *39*, 11519.
(44) (a) Li, W. J.; Hill, N. J.; Tomasik, A. C.; Bikzhanova, G.; West, R. *Organometallics* **2006**, *25*, 3802. (b) Mitra, A.; Wojcik, J. P.; Lecoanet, D.; Müller, T.; West, R. *Angew. Chem., Int. Ed.* **2009**, *48*, 4069.
(45) (a) Herber, R. H.; Nowik, I. *J. Organomet. Chem.* **2008**, *693*, 3007. (b) Herber, R. H.; Nowik, I. *J. Nucl. Radiochem. Sci.* **2008**, *9*, 33.
(46) Herber, R. H.; Nowik, I.; Cohen, S. *J. Phys.: Conf. Ser.* **2010**, *217*, 012145.
(47) Itazaki, M.; Kamitani, M.; Ueda, K.; Nakazawa, H. *Organometallics* **2009**, *28*, 3601.
(48) Herber, R. H. In *Chemical Mössbauer Spectroscopy*; Herber, R. H., Ed.; Plenum Press: New York, 1984; p 199 ff.
(49) Cohen, S.; Ma, J.; Butenschoen, H.; Herber, R. H. *Dalton Trans.* **2009**, 6606.
(50) (a) Gol'danskii, V. I.; Makarov, E. F. In *Chemical Mössbauer Spectroscopy*; Gol'danskii, V. I., Herber, R. H., Eds.; Plenum Press: New York, 1968; pp 102; (b) Greenwood, N. N.; Gibb, T. C. In *Mössbauer Spectroscopy*; Chapman and Hall: London, 1971; p 74.
(51) Lesley, G.; Nguyen, P.; Taylor, N. J.; Marder, T. B.; Scott, A. J.; Clegg, W.; Norman, N. C. *Organometallics* **1996**, *15*, 5137.
(52) *Apex II diffractometer control software*; Bruker Analytical X-ray Instruments Inc.: Madison, WI, 2007.
(53) Sheldrick, G. M. *SADABS: A program for absorption correction with the Siemens SMART system*; University of Göttingen: Germany, 1996.
(54) Sheldrick, G. M. *Acta Crystallogr.* **2008**, *A64*, 112–122.
(55) *International Tables for Crystallography*; Kluwer: Dordrecht, 1992; Vol C.